A. J. ACOSTA
Mem. ASME

T. KICENIUK
Mem. ASME

E. R. BATE, JR.
Hydrodynamics Laboratory,
Kármán Laboratory of
Fluid Mechanics and Jet Propulsion,
California Institute of Technology,
Pasadena, Calif.

Measurements on Fully Wetted and Ventilated Ring Wing Hydrofoils

Force measurements and visual observations were made in a water tunnel on fully wetted and ventilated flows past a family of conical ring wings having a flat plate section geometry. The diameter-chord ratio was varied from one to three, at a fixed total included cone angle of 12 deg. The fully wetted flows all exhibited separation from the leading edge except for the largest diameter-chord ratio, a result which has been attributed to excessive cone angle. The effect of ventilation is to reduce markedly the lift curve slope. Pressure distribution measurements were also made under ventilating conditions for one member of this series. The effect of ventilation over only a portion of the circumference of the ring was also briefly investigated; large cross forces were developed by such ventilation.

Introduction

THE GENERAL characteristics of ring wings in uniform flow are well known, having found application in marine propellers, aircraft, torpedoes, and depth bombs. The function and description of many of these applications are to be found in references [1 and 2],[1] while the general theoretical background of ring wings is dealt with in references [2 through 10].

All of the foregoing references and applications deal with fully wetted flow; that is, the surrounding fluid is either all liquid or all air. Because of the proximity of a neighboring free surface in a flow of liquid, or perhaps as a result of the deliberate injection of gas into a liquid flow, a two-phase flow may take place. The object of the present work is to study and to treat experimentally some of the problems associated with the use of superventilating and partly ventilating ring wings. The information thus gained may be useful for devising new schemes of direction control which may augment or replace altogether the conventional rudders found on ships or torpedoes. The possibility of such an application was originally suggested by Smith and later followed up in the work of Lang and Daybell [11] in water tunnel tests carried out at the California Institute of Technology on two-dimensional hydrofoils with controlled air ventilation.

[1] Numbers in brackets designate References at end of paper.

Contributed by the Underwater Technology Division and presented at the Winter Annual Meeting, New York, N. Y., November 27–December 1, 1966, of THE AMERICAN SOCIETY OF MECHANICAL ENGINEERS. Manuscript received at ASME Headquarters, June 16, 1966. Paper No. 66—WA/UnT-4.

Description of Apparatus and Experimental Technique

Facility Description. The experimental work described in this paper was performed in the Hydrodynamics Laboratory at the California Institute of Technology using the free-surface water tunnel. Reference [12] describes in some detail the facilities of the laboratory and, in particular, the operation of the free-surface water tunnel.

In the first test series, the measurements were made of the total forces acting on complete ring assemblies. To accomplish this, the ring models were held by a strut, which, in turn, was supported by a strain-gage balance, Figs. 1, 2. The balance was rigidly attached to "ground" above the water surface and the support strut held the model submerged in the flow. The objective of the second series of tests was to determine the pressure acting at various points on the model. A complete series of such measurements would yield the total pressure distribution on the

Nomenclature

A = area, total wetted area of ventilating models, one-half wetted area of fully wetted models

c = model chord (measured along cone generator)

C_D = drag coefficient, $\dfrac{D}{1/2\rho V^2 A}$

C_L = lift coefficient, $\dfrac{L}{1/2\rho V^2 A}$

$C_{L\alpha}$ = rate of change of lift coefficient with angle of attack

C_M = moment coefficient, $\dfrac{M}{1/2\rho V^2 A(2r_1)}$

C_n = normal force coefficient, $\dfrac{n}{1/2\rho V^2 \dfrac{A}{2\pi}}$

C_p = pressure coefficient, $\dfrac{p - p_\infty}{1/2\rho V^2}$

C_Q = airflow rate coefficient, $\dfrac{Q}{\pi(r_1^2 - r_2^2)V}$

D = total drag force

d = depth of model center line from water surface

F = Froude number, $V/\sqrt{2gr_1}$

k = ventilation number, $\dfrac{p_\infty - p_k}{1/2\rho V^2}$, also called cavitation number

L = total lift force

M = pitching moment about ring leading edge

n = normal force perpendicular to surface of conical ring per unit polar angle

p = static pressure measured at any point of body

p_k = cavity pressure

p_∞ = free-stream pressure far upstream of the model center line

Q = quantity of ventilating gas supplied at ambient pressure in the cavity

r = radius measured to any point on the model measured from the model center line

r_1 = radius at entrance of ring

r_2 = radius at exit of ring

$2r_1/c$ = model aspect ratio

V = velocity

x = distance of pressure tap location from leading edge of model

α = angle of attack of force model

Γ = bound circulation about chord of ring profile

γ = half-cone angle of conical models, 6 deg

θ = polar angle measured positive clockwise looking downstream from water surface

ρ = water density

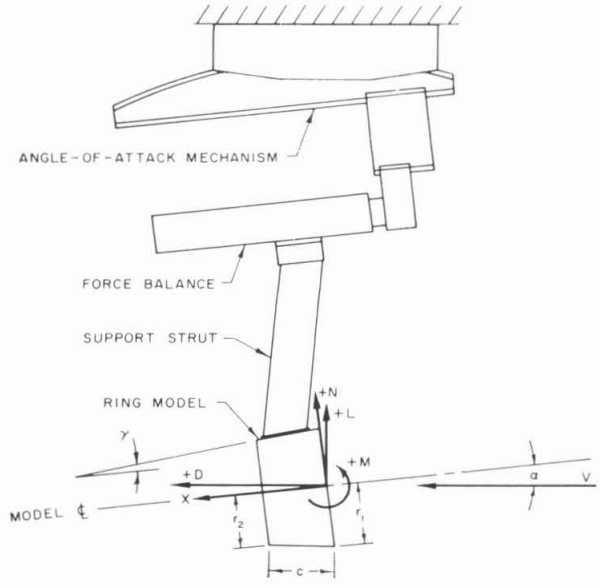

Fig. 1 Forces on ring wing showing sign convention and the force-measuring apparatus

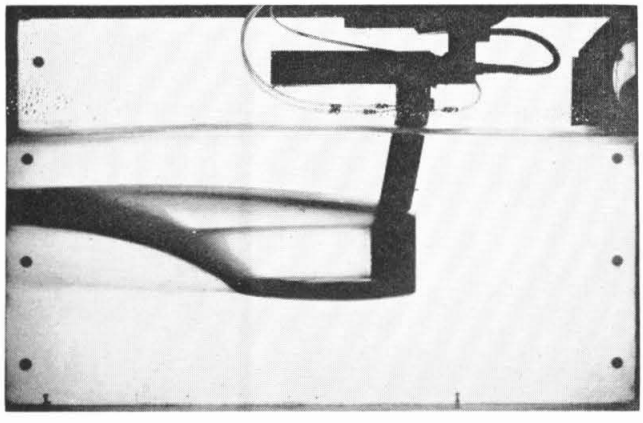

Fig. 2 Fully ventilated ring wing. The chord is 3 in. and the diameter 6 in. The cavitation number is 0.13 and the angle of attack is 0 deg.

model. To accomplish this, a rigid metal plate was mounted at the plane of the water surface. The surface of this plate provided a plane of symmetry for the flow and was hence called a "reflection" plane. In this way, the free-surface water tunnel was converted into a closed jet tunnel having a working section approximately 20 in. sq, Figs. 3, 4. The model in this case consisted of a half ring projecting through the reflection plane.

Cavity pressures were measured using a water manometer connected to a small hole drilled in the side of the model which communicated to the cavity. Air was bled slowly through the cavity pressure-measuring lines to insure that they would be free from water. This airflow resulted in a small zero offset in the cavity pressure readings which was accounted for in the data reduction process. The main cavity air supply rate was measured using a Fisher-Porter flowmeter and reduced to ambient conditions by applying the proper corrections for line pressure and temperature. The forces acting on the models were measured with a Task Corporation six-component electrical strain-gage balance and displayed on an integrating digital voltmeter. Individual pressure transducers were used to measure the pressure distribution, and the outputs of these pressure transducers were also monitored by the digital voltmeter.

To determine the pressure coefficients from the measurements made with the pressure distribution model, a detailed knowledge of the flow in the vicinity of the model was necessary. Both the boundary-layer thickness and the flow direction at the reflection plane near the model mounting location were measured. These surveys revealed that the boundary layer in the vicinity of the model is approximately $^1/_4$ in. thick and the flow deviation over the intercepted radius of the model is approximately 0.7 deg.

Model Description. Before deciding upon the final configuration of the ring model, it was thought advisable to perform a series of preliminary design experiments which would help decide questions of model size and geometry, both in the fully wetted and cavitating flow regimes. In addition, the proposed system for supplying air to the model in the cavitating case could be studied.

Several important considerations dictated the choice of model section:

(*a*) Because of the exploratory nature of these experiments, the model should be easy to fabricate so that various model sizes, aspect ratios, and so on, may be readily studied.

(*b*) The model should be able to operate fully wetted and fully ventilated, as well as partially ventilated, without changing its effective geometry; i.e., cone angle, camber, or attachment point of cavity.

(*c*) The results should be amenable to comparisons with theory and past experiments, both to those pertaining to ring wings and to two-dimensional airfoils.

For these reasons, the test model was constructed in the form of a cone having a total included angle of 12 deg, as a cone is the simplest configuration that provides a normal force in axisymmetric flow. The section profile consisted of a $^1/_8$-in-thick flat plate with a rounded semicircular nose and blunt trailing edge. Air was supplied to the cavity by means of a small slit approximately 0.005 in. wide, machined in the brass model on the suction side at the point of tangency between the cylindrical leading edge and the flat surface, Fig. 5. The slit was connected to a plenum chamber machined into the flat plate section and to the laboratory air supply by tubes which ran up the inside of the hollow support strut.

The upstream, or inlet, diameter of the cone was fixed at 6 in. for both the force model in Fig. 2 and the pressure distribution "half model" in Fig. 4. To investigate the effect of changes in model chord, the force model was constructed of a main ring and a series of trailing edge adapter rings, Fig. 5, resulting in models of 2, 3, 4, and 6-in. chord. The pressure distribution model was fabricated in the 3-in. chord size only.

A cylindrical model having a 3-in. chord and without provisions for air ventilation was also made for measuring the forces under fully wetted conditions.

Force Measurements. The forces acting on the ring models were measured using the strain-gage balance. The model-strut assembly is attached to the force balance, which is, in turn, supported by the angle-changing mechanism with rotation taking place about a center arranged to coincide with the center line of the model. Since the balance rotates with the model, the forces are measured with respect to the model axes. These forces are subsequently referred to as axes parallel to the undisturbed flow upstream.

Although the strain-gage balance is capable of measuring six force components, only those necessary to determine lift, drag, and pitching moment were actually taken as data; the other three were only monitored to insure proper yaw alignment.

For the case of the cavitating models, the cavity air supply was determined for each configuration that would give a fully developed cavity over the entire range of angles of attack. The air supply rate was then readjusted to this constant value before each data point was taken. The cavity pressure was measured and the variation in cavitation number at constant air supply for each of the test conditions is shown in Fig. 6. For the pressure distribution tests, air supply was not measured but cavity

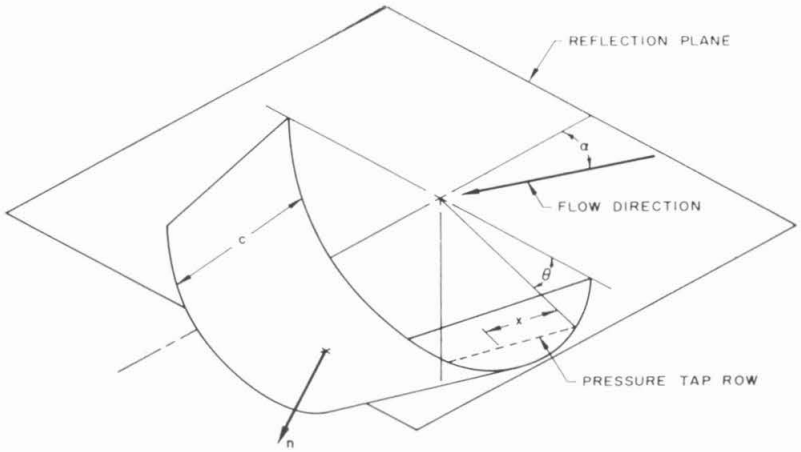

Fig. 3 Pressure distribution model schematic, defining the pertinent parameters and sign conventions

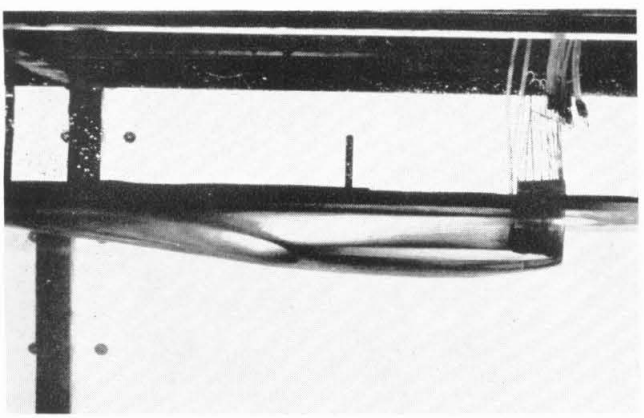

Fig. 4 Reflection plane mounted pressure distribution model. Chord is 3 in., $k = 0.10$, angle of yaw is 4 deg. Flow velocity is 18.6 fps.

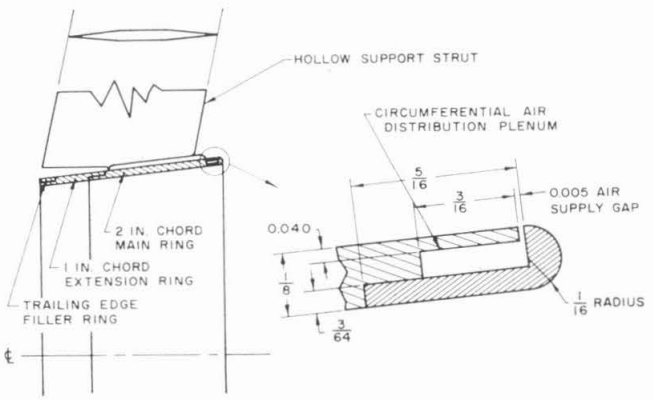

Fig. 5 Sketch showing assembly ring wings and the ventilation slot at the leading edge

pressure was taken as data. Here, two distinct values of cavitation number were obtained. One occurred when the cavity length was adjusted to approximately three body dia, and the other occurred when the cavity was allowed to grow until it extended beyond the plate and opened to the atmosphere, through the free surface. In the former case the cavitation numbers obtained were on the order of $k = 0.10$, and in the latter case they were approximately $k = 0.01$.

To minimize any possible interference between the model supporting strut and the ring wing itself, it was necessary to keep the thickness of the strut at an absolute minimum consistent with the requirements of strength and the geometrical arrangement of the tubes which supplied the ring with ventilating air and measured the cavity pressure. The present strut was made by an electroforming process in which nickel was deposited over a mandrel fashioned of a low-melting-point alloy. The mandrel which was subsequently melted out incorporated all the necessary tubes and mounting fixtures.

Pressure Distribution Measurement. In order to obtain detailed information about the local force coefficients on the ring wing in both cavitating and fully wetted flow, a pressure distribution model was employed with which the pressure at any desired location on both the pressure and suction surfaces of the model could be measured. For the purpose of this series of tests, the reflection plane previously mentioned was installed at the water surface in the free-surface water tunnel. The model was set in a mounting disk which, in turn, was itself placed in a large circular hole in the reflection plane. The lower surface of the mounting disk was

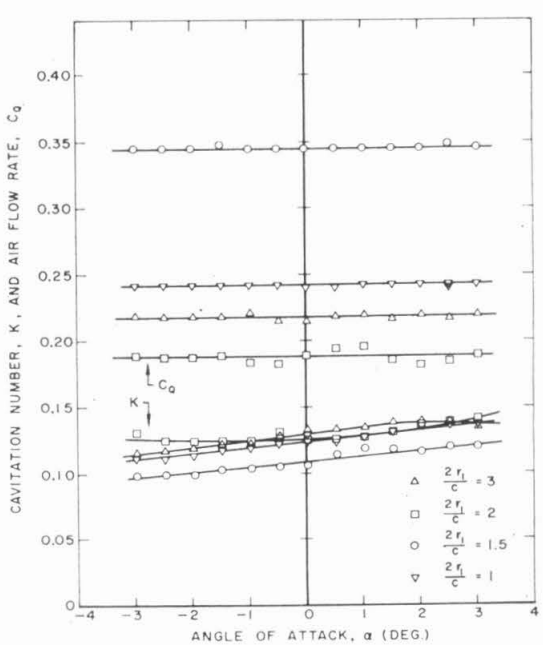

Fig. 6 Variation of measured cavitation (ventilation) number at fixed air supply rates for conical ring wings at varying aspect ratios

coincident with that of the reflection plane, Fig. 4. The disk could be turned about a vertical axis, thereby yawing the model with respect to the oncoming flow. Because of symmetry, this was equivalent to varying the angle of attack of a complete ring. A row of 11 pressure taps was drilled on both the pressure and suction surfaces of the model in a chordwise direction. These holes communicated to a corresponding number of $^1/_{16}$-in-dia brass tubes which were placed circumferentially in slots turned in the surface of the model. These tubes broke out of the surface of the model for subsequent attachment to lines leading to the pressure measuring transducers at a point approximately 150 deg around the ring from the location of the pressure taps. The chordwise pressure distributions were obtained directly by measuring the pressures at each of the different tap locations and the variation of pressure as a function of polar angle (or "spanwise" variation) could be determined by rotating the model about its central axis in the mounting disk which was set in the reflection plane. The pressure taps, however, could only be rotated from 0–120-deg polar angle. Pressure distributions around the complete ring were obtained when it was yawed by performing part of the measurements (0–90 deg) at a positive yaw angle and the remainder (90–180 deg) with a negative yaw angle. Fig. 3 shows the geometry of the pressure distribution model in schematic form.

Prior experiments performed on the complete ring used in the force measurements indicated that a fully ventilated condition could be maintained without using the leading edge slot but with the use of an auxiliary air supply, although injection of air through a leading edge slot was generally required to initiate ventilation. Because of the comparative complexity of the pressure tap model, the leading edge ventilation slot was omitted and ventilation was initiated by imparting large yaw angles to the model. Once started, the ventilation could be maintained through small air supply ports in the image plate located near the trailing edge of the ring even though the angle of yaw of the ring was subsequently reduced.

Tunnel Corrections. All of the data taken for the force measurements were corrected for strut tare forces. To accomplish this, the model was connected to an image support system attached to the floor of the tunnel. The image strut could be rotated, in a fashion similar to that of the main support strut, so that the model angle of attack could be changed about the model center. For determining the tare forces acting on the strut, only the 3-in. model was used over the same angle of attack range obtained in the force runs and the model was run both fully wetted and ventilated. For the cavitating case, cavity air was supplied through the main support strut, except that the air to the leading edge slit on the ring model was supplied by a hole drilled through the image strut and connected to the laboratory air supply by means of polyethylene tubing connected to the image strut and trailing downstream in the flow to a point where it was brought out through the free surface. The strut tare forces were determined with the strut held in approximately the same position relative to the model as it would have been during a normal force run, except that a small gap (about 0.050 in.) was left between it and the model. Weight and buoyancy tare forces were also obtained as a function of angle of attack for all of the models by swinging the balance and support strut with the various models attached through the angle of attack range both in air and at operating depth in still water.

The tare forces were obtained at the standard operating depth of 0.675 ft and at the standard operating tunnel speed of 18.56 fps only, then corrected for differences in velocity and wetted area before applying to the measurements.

Interference forces owing to the presence of the support strut in the fully wetted case were determined by holding the model by the support strut in the normal way and noting the change in the forces as the model was brought near the image strut. The interference corrections obtained in this manner were not applied to the original data, however, both because of the small values

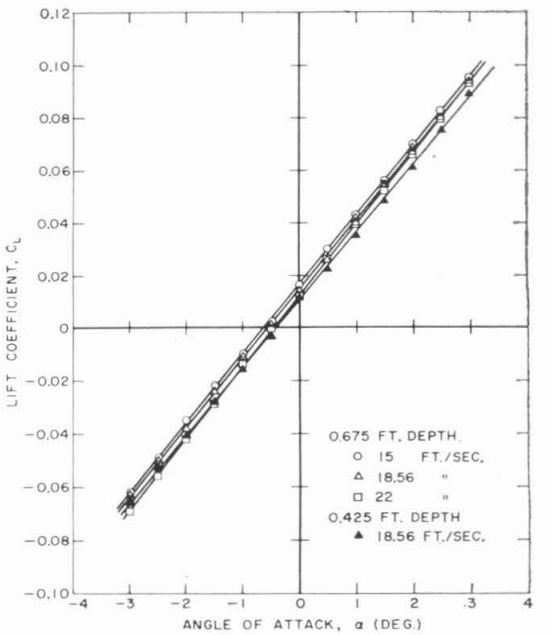

Fig. 7 The effect of velocity and submergence on the lift coefficient of a 6-in-dia cylindrical ring wing with 3-in. chord

obtained and because of the questionable validity of applying interference data obtained with a model having a 3-in. chord to the other models tested in this series.

Discussion of Results

Overall Forces. The results of the overall force measurements are presented in Figs. 7 through 10. In order to compare the present experimental results with previous analytical and experimental work, some tests were performed using a cylindrical model having a 6-in. dia and a 3-in. chord. These tests were also designed to isolate the effects of the tunnel velocity and the free surface in the absence of such complicating factors as model cone angle, flow separation, and so on, and hence these tests were performed at three values of the velocity and two different submergences. It can be seen from Fig. 7 that the main effect of velocity (or more probably Froude number) is to cause a slight shift in the angle for zero lift (about $^1/_4$ deg). Since the rings are relatively close to the surface, it is possible that the proximity of the free surface may have an effect on the forces experienced by the ring. It was not possible to answer this question exhaustively, owing to the geometric limitations of the working section. However, tests made on the cylindrical ring at a somewhat reduced submergence (0.425 ft) show only minor changes in the model forces. The slope of the lift curve is reduced approximately 4 percent and the angle for zero lift is shifted by about $^1/_4$ deg. On the basis of these findings the subsequent experiments, except where noted, were carried out at a standard tunnel speed of 18.56 fps and at a standard submergence of 0.675 ft or 1.22 ring dia to the model center line. Because of the effect of gravity on the free surface of the tunnel and on the cavity formed during the ventilation experiments, it can be expected that the Froude number will be a significant modeling parameter. To vary the Froude number without encountering severe problems of either tunnel blockage or real fluid effects predominant at small Reynolds numbers would require a much larger working section. It is interesting to note, however, that the standard model test conditions, i.e., 18.56 fps and 6-in. ring dia, would correspond to a 21-in-dia ring wing at a speed of 20.6 knots. This figure lies in the range of possible prototype applications.

Experimental results for the conical rings are shown in fully

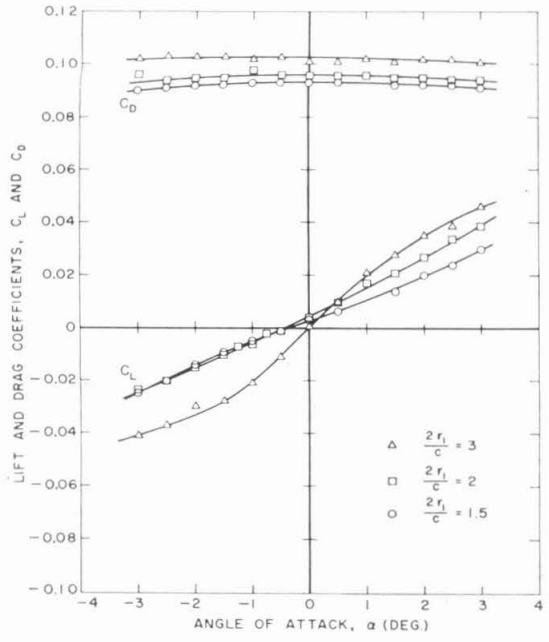

Fig. 8 The effect of aspect ratio on the lift and drag coefficients of a fully wetted ring wing with 12 deg included cone angle. The velocity is 18.5 fps.

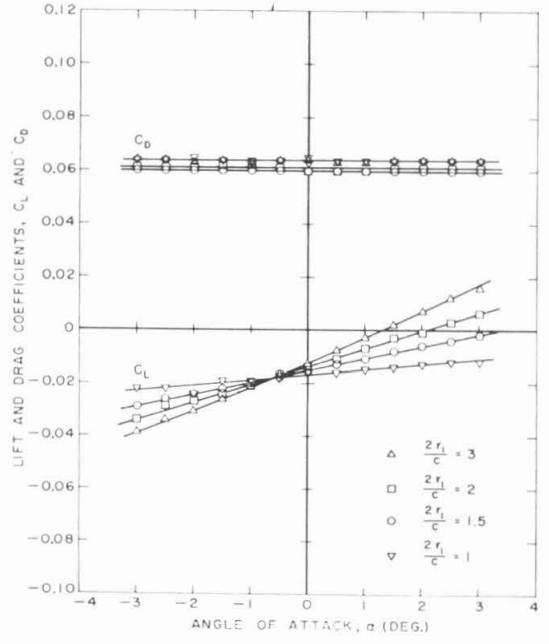

Fig. 9 The effect of aspect ratio on the lift and drag coefficients of a fully ventilated ring wing with a 12 deg included cone angle. The velocity is 18.5 fps.

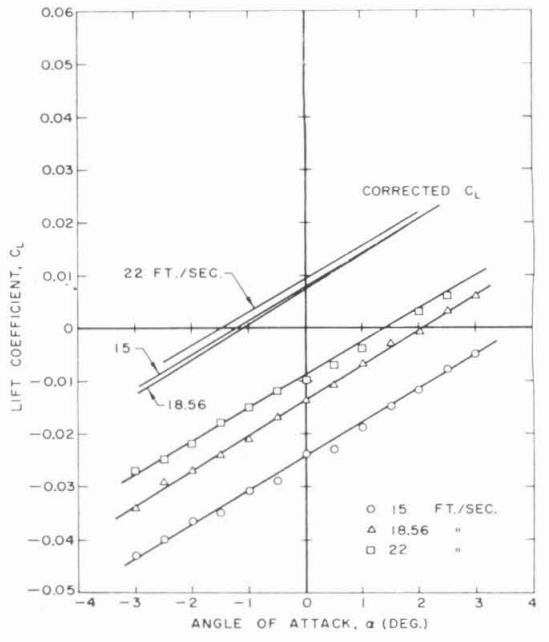

Fig. 10 Lift coefficient versus angle of attack for the 3-in. cone at various tunnel velocities or Froude numbers in fully ventilated flow. (The lines labeled "corrected C_L" are the same as each of the experimental curves except that the weight of the water contained by the wing has been subtracted from the lift force.)

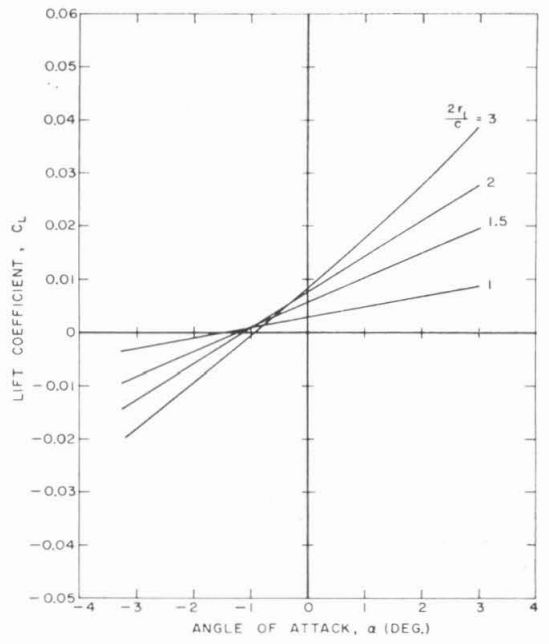

Fig. 11 Lift coefficient versus angle of attack for the family of cones in fully ventilated flow corrected for the weight of water contained within the volume of the ring. Tunnel velocity is 18.56 fps.

wetted flow in Fig. 8 and in fully ventilated flow in Fig. 9. The slopes of the lift curves are higher for the fully wetted results than for the ventilating, though not by much. Fig. 10 shows the effect of Froude number (or tunnel velocity) on the ring of aspect ratio two. The angle for zero lift is markedly Froude number dependent. Since the interior of the ventilated ring is filled with water and the outside of the ring is exposed to the constant pressure of the cavity, a major portion of the observed lift must be the result of the weight of the enclosed liquid. The force due to this liquid was reduced to coefficient form for each of the test velocities and subtracted from the observed lift coefficients, a procedure which tends to make the resultant curves coalesce. The data shown in Fig. 9 have been similarly corrected and presented in Fig. 11. The curves thus obtained still do not show zero lift at zero angle of attack and, indeed, this zero lift angle does not remain exactly constant for the various rings and tunnel velocities. This is to be expected since the effect of gravity on the cavities, Fig. 2, is to produce a pronounced ver-

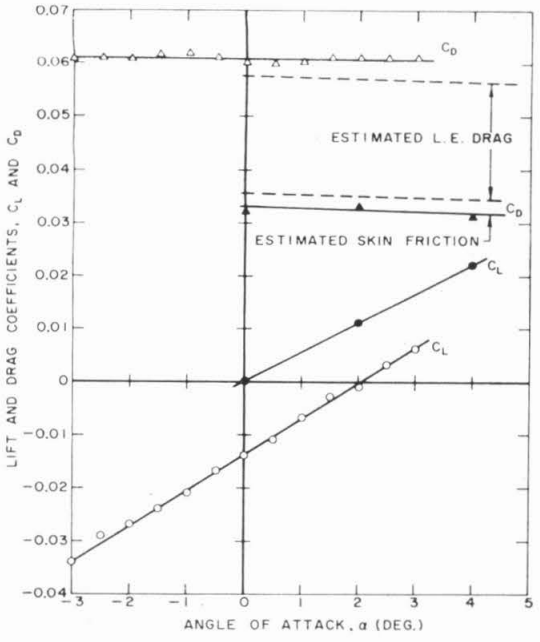

Fig. 12 Comparison of 3-in-chord, fully ventilated ring with results of the pressure distribution model. The solid points are the result of calculations made from measured surface pressures on the model.

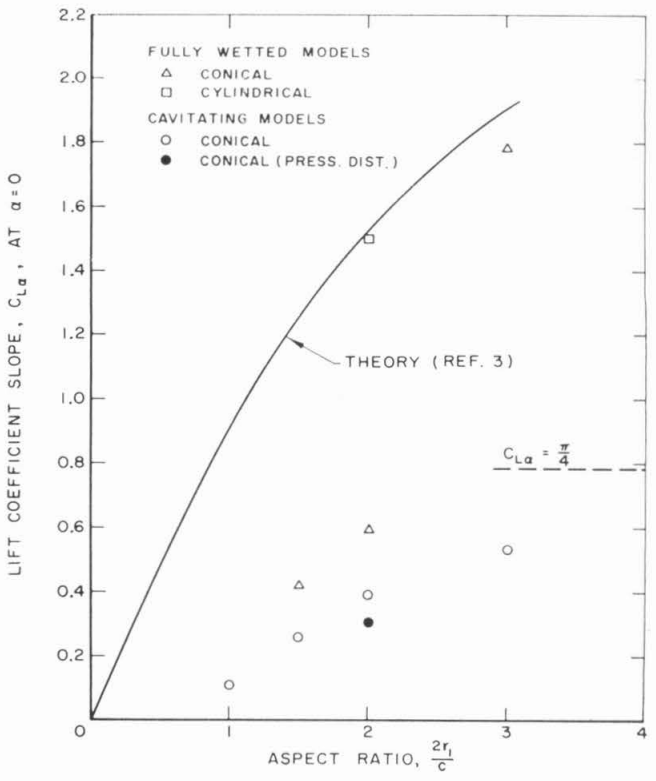

Fig. 13 Lift slope values for the measured ring wings in fully wetted and ventilated flow. (Data were obtained with both the force models and the pressure distribution model.) Velocity is 18.56 fps.

tical asymmetry, while blockage of the flow by the cavity distorts the free surface of the water in the tunnel. It is not yet possible to distinguish these two effects experimentally; nevertheless, the weight of the water contained within the ring contributes a major effect.

The results of the pressure distribution measurements which will be presently discussed are compared with the full ring measurements for the 3-in. (aspect ratio two) ring in Fig. 12. These results, on the whole, agree well though they are not identical. This is undoubtedly the result of the two different effects; the direction of gravity in respect to the definition of angle of attack is different in the two types of measurements. From Figs. 1 and 3, as well as the photographs in Figs. 2 and 4, it can be seen that nothing corresponding to the weight of the enclosed liquid could arise in the pressure distribution measurements. However, the two lift slopes are different too. This can be explained again by the different orientation of the gravity force and also by the different conditions prevailing for tunnel interference for the reflection plane mountings. Pressure distributions alone do not permit the determination of either frictional drag or of leading edge drag in ventilation conditions (the latter because severe space limitations prohibit placing a sufficient number of pressure taps on the small leading edge). Calculations were made of the flat plate friction drag at the appropriate Reynolds number as well as for the leading edge pressure drag. This leading edge drag was assumed to be the same as on a circular cylinder with the same diameter as the leading edge and with a length equal to the circumference of the ring. These estimates, Fig. 12, agree quite well with the measured drag force on the 3-in. ring.

The slopes of the lift coefficient curves at zero angle of attack are summarized in Fig. 13 for all of the rings tested. It can be seen that the fully wetted models of aspect ratios 1.5 and 2 approach fairly closely the performance of the ventilated rings, suggesting strongly that they are, in fact, subjected to separation resulting in a flow resembling ventilated flow except for a different "cavity" pressure. The highest aspect ratio fully wetted conical ring approached Weissinger's theoretical values [3], and the cylindrical ring is very close to his theory. Visual observations on the conical ring of aspect ratio three with small tracer bubbles of air showed that the separation bubble at the leading edge re-

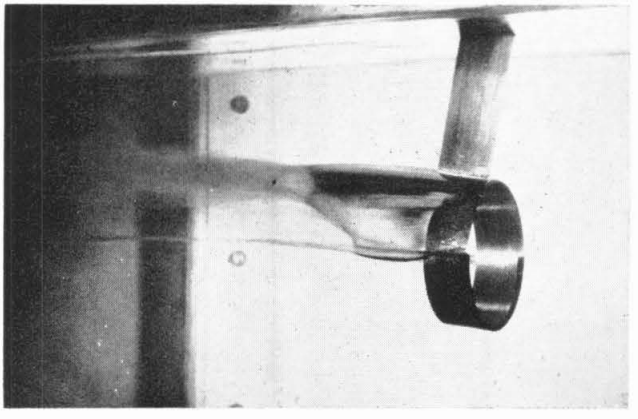

Fig. 14 Selective ventilation over one half the periphery of the ring for the 2-in. chord. (To prevent ventilation around the entire ring, small auxiliary "fences" are used.)

attached itself to the surface of the cone ahead of the trailing edge, so that values of lift slope should be near the theoretical value, as indeed they were.

The lift slope values for the fully ventilated cases appear to approach the value of $\pi/4$ as the aspect ratio becomes large. It is easy to show that this limit is the correct one for a ring wing of infinitesimal chord and small cone angle at zero cavitation number. It is, in fact, precisely one quarter of the lift slope for the fully wetted ring of infinite aspect ratio and, as is well known, for small angles of incidence to the flow a cavitating flat plate hydrofoil at zero cavitation number has one quarter the lift of a fully wetted hydrofoil. The actual ratios of the ventilated lift slopes to those of the fully wetted theory of Weissinger are 0.28,

0.29, and 0.19 for the aspect ratios of 3, 2, and 1.5, respectively. All of these vented flows have cavitation numbers somewhat higher than zero, Fig. 16, and can therefore be expected to show a small increase in the lift slope.

Selective Ventilation. The foregoing experiments all deal with a basically axisymmetric flow. Two experiments were carried out in which only a portion of the circumference of the ring was ventilated, Fig. 14. Because the flow past these rings is separated near the leading edge of the cone when fully wetted, the ventilation gas tended to migrate around the full circumference. This migration was prevented by the attachment of fins or fences aligned with the free-stream direction and only large enough to span the cavity at the ring. The resultant cross force owing to the partial ventilation is shown in Fig. 15 for both the 2 and 3-in. rings. It can be seen that the magnitude of the force developed by the partial ventilation is equivalent to an angle of attack of about 12 deg on an entire fully wetted ring. The resulting vertical force is directed downward for the ventilating condition shown in Fig. 14.

It should be remarked that had the basic ring foils not been separated near the leading edge, there would have been no necessity for the ventilation fences, as was found to be the case in reference [11]. The fences contribute a lift force opposite in direction to the developed cross force, so that the results in Fig. 15 are at least conservative.

Pressure Distributions. Pressure distributions on the ring of aspect ratio two are shown in Figs. 16 to 18. They include fully wetted flows and two different cavitation (or ventilation) numbers in the

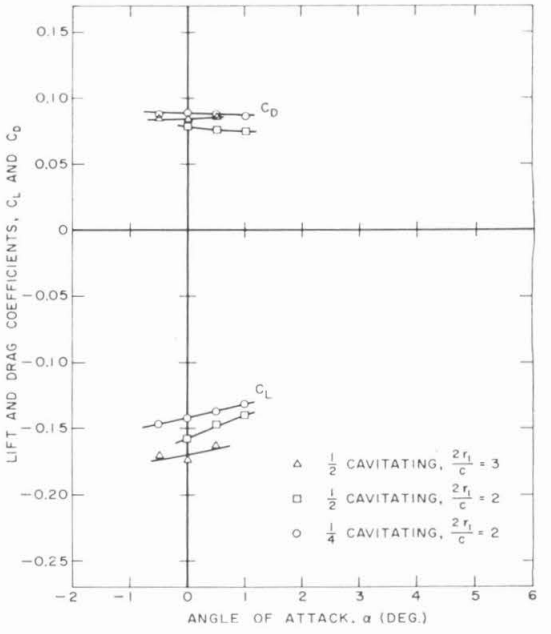

Fig. 15 The effect of ventilating part of the ring circumference on the forces in the vertical plane for ring wings of several aspect ratios

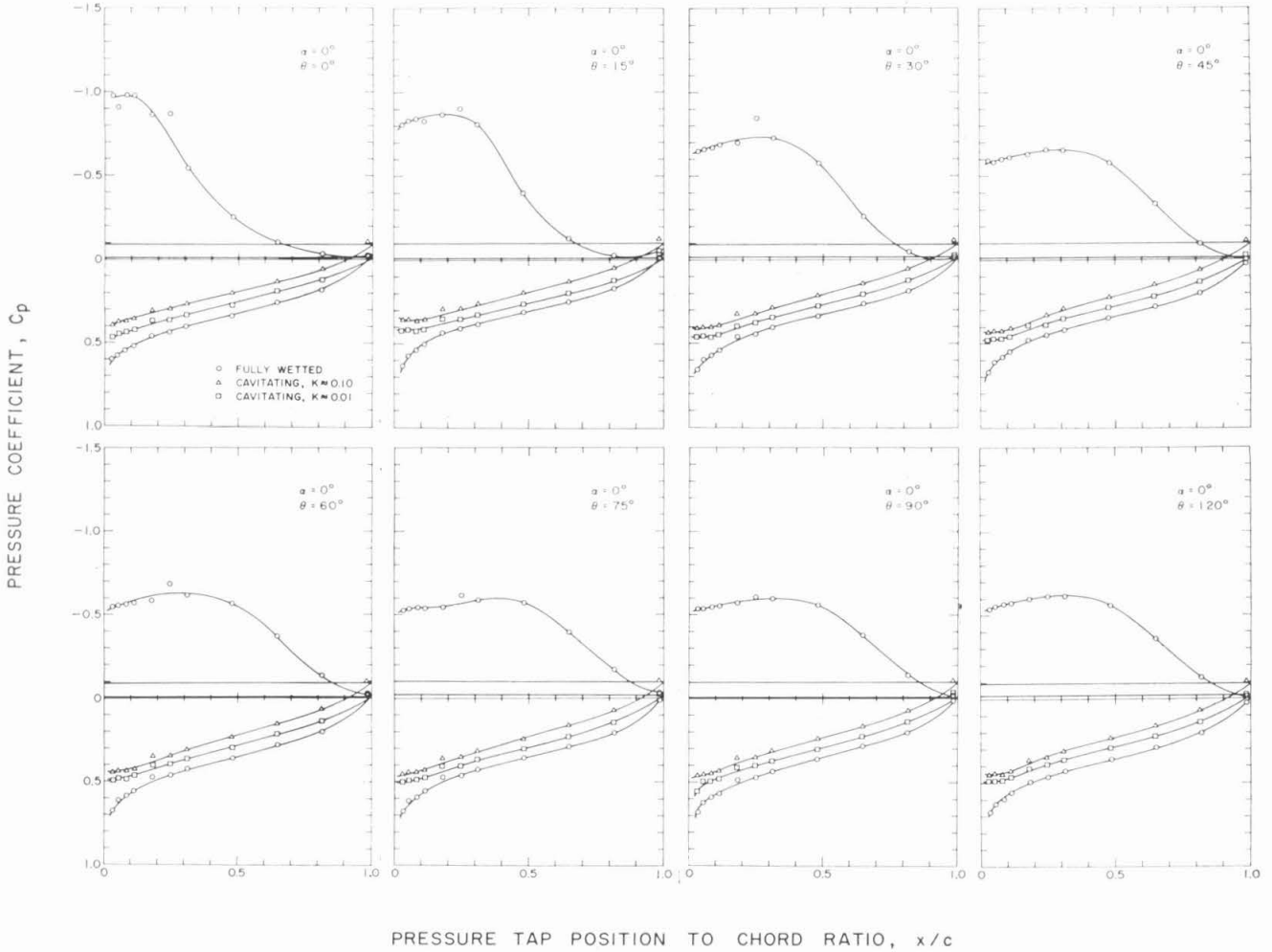

Fig. 16 Pressure distributions at various polar angles around a conical ring of aspect ratio two for fully wetted flow and ventilated flow at two cavitation numbers. Angle of attack is 0 deg. The horizontal lines above the axis in each of the figures indicate the pressure within the ventilated cavity.

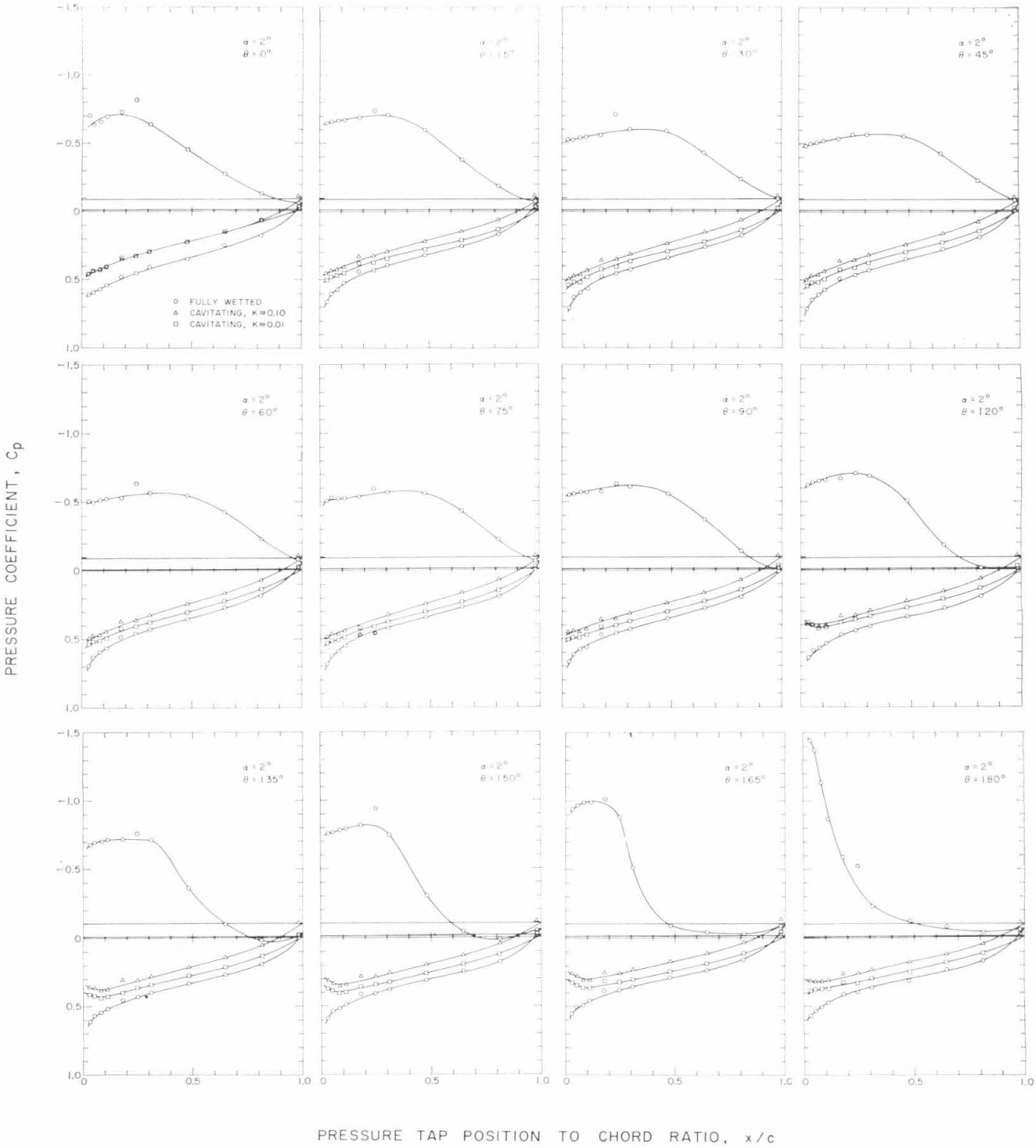

Fig. 17 Pressure distributions at various polar angles around a conical ring of aspect ratio two for fully wetted flow and ventilated flow at two cavitation numbers. Angle of attack is 2 deg. (Experimental points at polar angles greater than $\theta = 120$ deg were obtained at negative angle of attack.)

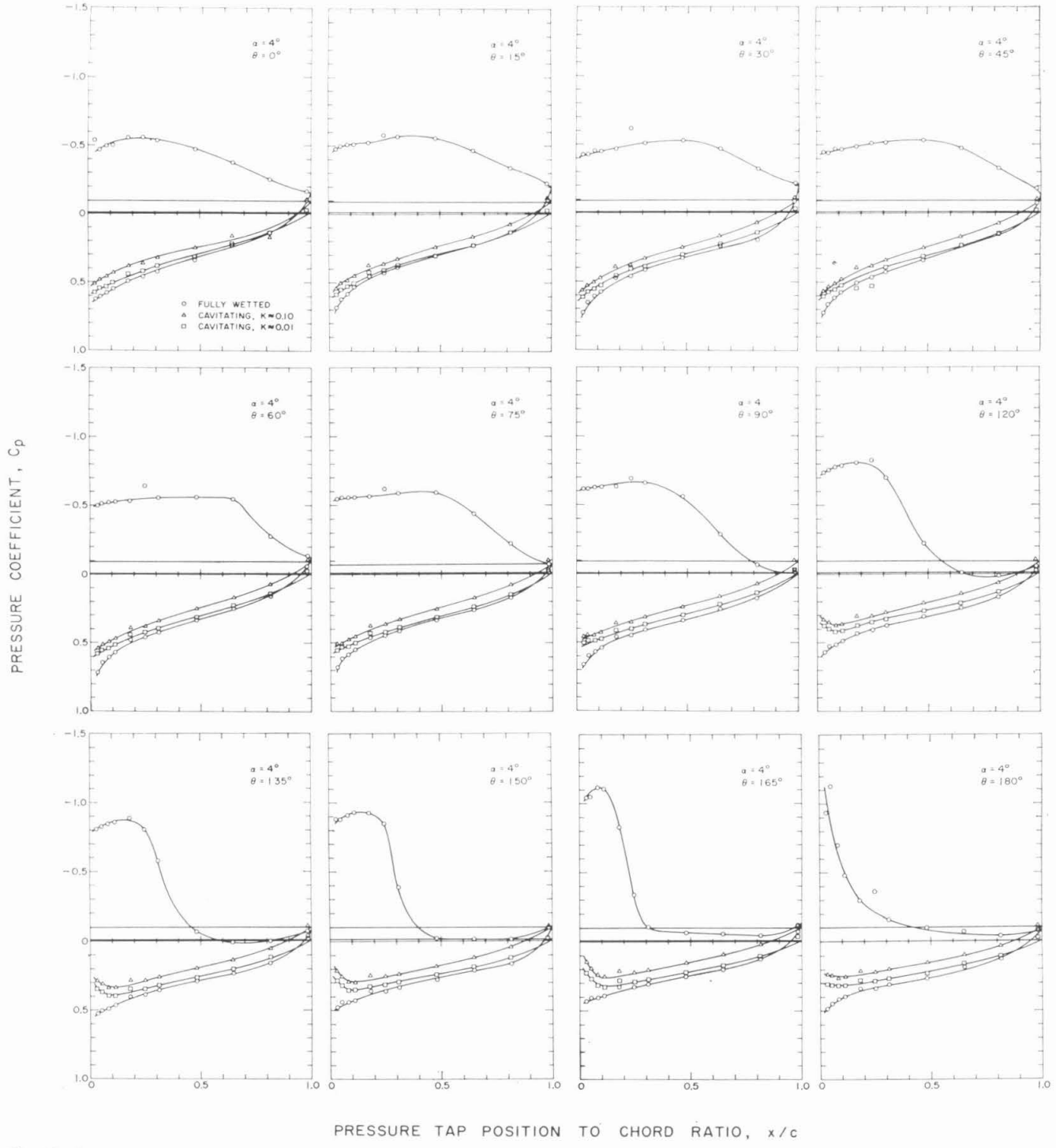

Fig. 18 Pressure distributions at various polar angles around a conical ring of aspect ratio two for fully wetted flow and ventilated flow at two cavitation numbers. Angle of attack is 4 deg. (Experimental points at polar angles greater than $\theta = 120$ deg were obtained at negative angle of attack.)

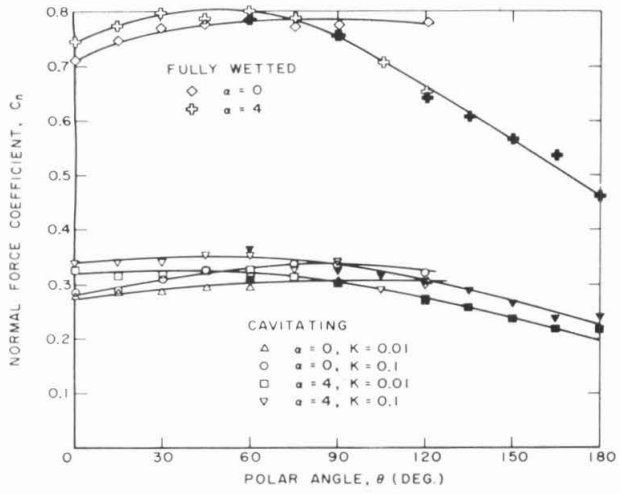

Fig. 19 Radial force coefficients as a function of polar angle around a conical ring wing for fully wetted flow and ventilated flow for two angles of attack. The diameter-chord ratio is 2.0 and the half angle of the cone is 6 deg. The solid symbols represent data obtained at negative angles of attack.

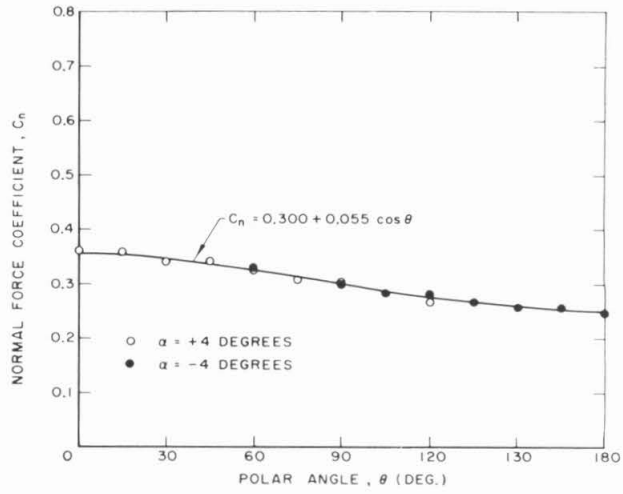

Fig. 20 Normal force coefficient versus polar angle for a ventilated ring wing of 2.0 diameter-chord ratio corrected for effects of tunnel swirl. The cavitation number is 0.01 and the angle of attack is 4 deg.

ventilated condition. Pressure distributions are shown for several polar angles θ around the ring, as sketched in Fig. 3. The appearance of these plots strongly suggests the existence of large regions of separation for the fully wetted flows, especially at the largest angle of attack.

Each of the pressure distribution curves was numerically integrated to give a local normal force coefficient as a function of the polar angle around the ring, and these were then plotted as a function of the polar angle, as shown in Fig. 19. The effects of the tunnel swirl can clearly be seen in this figure by examination of the curves for the normal force coefficient at zero angle of attack. If there had been no swirl, these lines should be horizontal and independent of polar angle. The amount by which they deviate from a horizontal line drawn through their maximum point (which occurs at a polar angle of 90 deg) indicates the effect of the swirl at each polar angle. The effect of the tunnel swirl on the normal force coefficients can be eliminated at all other angles of attack by adding to them this incremental difference at each polar angle. (This tacitly assumes a linear behavior of force coefficients with local flow angle.) This was done for one of the cavitating runs and a diagram of normal force coefficient versus polar angle which has been corrected for swirl at an angle of attack of 4 deg and a cavitation number of 0.01 is shown in Fig. 20. This distribution is well-fitted by a cosine curve. Velocity distributions were calculated from the pressure distributions, the effect of swirl being treated as in the foregoing. From these, the distribution of bound circulation was calculated and is shown in Fig. 21. Within the accuracy of these calculations, this curve is again adequately fitted by a cosine curve. Such a distribution gives rise to an upwash consistent with the ring acting as a minimum induced drag lifting surface [4].

With this information, it is of interest to see if an estimate can be made of the effective lift slope of a two-dimensional hydrofoil section which would be needed in a strip theory calculation of the properties of the lifting ventilated ring. In a fully wetted ring of small chord-diameter ratio we should, of course, get 2π, the lift slope of an isolated fully wetted hydrofoil, as this is the basis of Ribner's theory. Calculation of the effective incidence to the local hydrofoil sections requires knowing the induced radial inwash around the hydrofoil. This depends upon the circumferential distribution of bound circulation and additional terms resulting from the presence of nonaxisymmetric ventilated cavity. These are relatively difficult to evaluate; in what follows, we will estimate the distribution of radial inwash from the bound circulation alone. It can be shown that the radial inwash angle owing to a sinusoidal polar distribution of bound circulation of amplitude $\Delta\Gamma$ is 57.3 $\Delta\Gamma/2Vc$ deg. The difference in local incidence to the section of the ring between 0 and 90 deg polar angle (with reference to Fig. 21) is thus $4 - 57.3\ \Delta\Gamma/2Vc = 2.997$ deg. The corresponding variation in normal force coefficient is obtained from Fig. 20, from which we can determine that the effective value of $dC_L/d\alpha$ would be

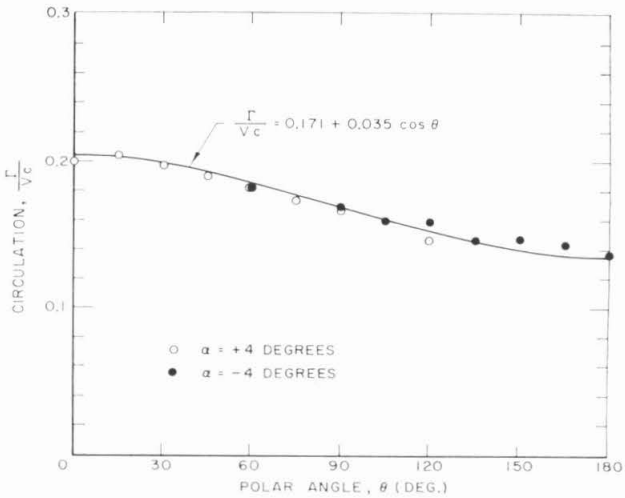

Fig. 21 Distribution of circulation around the ventilated ring wing in Fig. 20

$$dC_L/d\alpha = 0.055/(2.997)/(57.3) = 1.02$$

Had the hydrofoil sections acted as two-dimensional ventilated hydrofoils in a free stream, we would have gotten the well-known result that the lift slope would be $\pi/2 = 1.57$, which is considerably higher than that estimated. Also, it is worth noting that the overall lift slope of the ring as measured from pressure distributions, Fig. 13, 0.3, is only 19.8 percent of Ribner's theory. If the ventilated ring were to act as in Ribner's theory with no account taken of effect of the cavity on local radial inwash, an effective lift slope of the profile sections of $(0.198)(2\pi) = 1.24$ would be required which is still some 20 percent higher than that estimated from the present data. Although these numbers are

somewhat speculative, they do suggest at the very least that additional downwash effects arising from the axisymmetric cavity should be accounted for in such flows; it is also possible that a complete lifting surface theory accounting for the cavity and wetted surface in detail may be required for a full explanation. It is likely that such "source" effects resulting from the presence of a cavity will be even more important for selective ventilation.

As mentioned in an earlier section, the axisymmetric cavity problem has yet to be solved for the present configuration. A related problem is the cavitating two-dimensional flow past a flat plate near the ground. The flows are similar except that the one is a plane flow and the other is axisymmetric. Values of $dC_L/d\alpha$ have been computed for the plane flow at zero cavitation number [13]. The two-dimensional values give a value for this parameter of about 2.4. The corresponding values for zero angle of attack on the ring can be estimated from Fig. 19 by dividing the average normal force coefficient by the local angle of incidence of the ring; namely, 6 deg. This gives a value of $dC_L/d\alpha$ equal to 2.8, which is in quite reasonable agreement with the two-dimensional value.

Acknowledgments

The authors would like to acknowledge the help of the laboratory staff and would especially like to mention the efforts of Messrs. L. Whitcanack, W. Wilson, and C. Eastvedt in carrying out the experiments. They would further like to acknowledge the suggestions of Mr. O. Seidman in reviewing the manuscript. This work was supported by the Office of Naval Research under Contract Nonr 220(54) and administered under the technical direction of the Bureau of Naval Weapons, Fluid Mechanics and Flight Dynamics Branch, Code RRRE-4.

References

1 A. H. Sacks and J. A. Burnell, "Ducted Propellers—A Critical Review of the State of the Art," Advanced Research Division of Hiller Aircraft Corporation, Report No. ARD 232, June 26, 1959.

2 J. Levy and R. T. Knapp, "Water Tunnel Tests of the MK 13-1, MK 13-2 and MK 13-2A Torpedoes With Shroud Ring Trails," California Institute of Technology, HML Report No. ND-15.1, November 24, 1943.

3 J. Weissinger, "Some Results From the Theory of the Ring Wing in Incompressible Flow," *Trans. From Advances in Aeronautical Sciences, Proceedings of First International Congress in the Aeronautical Sciences*, Madrid, Spain, September 8–13, 1958, vol. 2, pp. 798–831.

4 Herbert S. Ribner, "The Ring Wing in Nonaxial Flow," *Journal of Aeronautical Sciences*, vol. 14, 1947, p. 529.

5 A. R. Kriebel, A. H. Sacks, and J. N. Nielsen, "Theoretical Investigation of Dynamic Stability Derivatives of Ducted Propellers," Vidya Report No. 63-95, January 9, 1963.

6 A. R. Kriebel, "Theoretical Investigation of Static Coefficients, Stability Derivatives, and Interference for Ducted Propellers," Vidya Report No. 112, March 31, 1964.

7 A. R. Kriebel, "Theoretical Stability Derivatives for a Ducted Propeller," Vidya Interim Report, October 18, 1963.

8 A. R. Kriebel, "Interference Between a Hull and a Stern-Mounted Ducted Propeller," Vidya Report No. 161, September 30, 1964.

9 J. Weissinger, "Ring Airfoil Theory, Problems of Interference and Boundary Layer," Institut für Angewandte Mathematik der Technischen Hochschule, Karlsruhe, Germany, January, 1959.

10 J. F. Reynolds, "Lifting Surface Theory Applied to Isolated Ring Wings at Angle of Attack," NAVWEPS Report 8401, NOTS TP 3322, November, 1963.

11 T. G. Lang and D. A. Daybell, "Water-Tunnel Tests of Three Vented Hydrofoils in Two-Dimensional Flow," *Journal of Ship Research*, vol. 5, no. 3, December, 1961.

12 R. T. Knapp, J. Levy, J. P. O'Neill, and F. B. Brown, "The Hydrodynamics Laboratory of the California Institute of Technology," TRANS. ASME, vol. 70, 1948, pp. 437–457.

13 D. K. Ai, A. J. Acosta, and Z. L. Harrison, "Linearized Theory of a Two-Dimensional Planing Flat Plate in a Channel of Finite Depth—I," California Institute of Technology, Hydrodynamics Laboratory Report No. E-110.2, April, 1964.

Reprinted from the August 1967
Journal of Engineering for Industry